A biofilm-tropic *Pseudomonas aeruginosa* bacteriophage uses the exopolysaccharide Psl as receptor

Brenna Walton[1)], Serena Abbondante[2,3)], Michaela Ellen Marshall[2,3)], Justyna M. Dobruchowska[4)], Amani Alvi[1)], Larry A. Gallagher[5)], Nikhil Vallikat[1)], Zhemin Zhang[8)], Daniel J. Wozniak[6,7)], Edward W. Yu[8)], Geert-Jan Boons[4,9,10)], Eric Pearlman[2,3)], Arne Rietsch[1,11)]

1) Dept. of Molecular Biology and Microbiology, Case Western Reserve University, Cleveland, OH, U.S.A.
2) Dept. of Ophthalmology, University of California, Irvine, CA, U.S.A.
3) Institute of Immunology, University of California, Irvine, CA, U.S.A.
4) Dept. of Chemical Biology and Drug Discovery, Utrecht Institute for Pharmaceutical Sciences, and Bijvoet Center for Biomolecular Research, Utrecht University, Utrecht, NL
5) Dept. of Microbiology, University of Washington, Seattle, WA, U.S.A.
6) Dept. of Microbial Infection and Immunity, The Ohio State University, Columbus, OH, U.S.A.
7) Dept. of Microbiology, The Ohio State University, Columbus, OH, U.S.A.
8) Dept. of Pharmacology, Case Western Reserve University, Cleveland, OH, U.S.A.
9) Complex Carbohydrate Research Center, University of Georgia, Athens, GA, U.S.A.
10) Dept. of Chemistry, University of Georgia, Athens, GA, U.S.A.
11) Corresponding author: arne.rietsch@case.edu

Abstract

Bacteria in nature can exist in multicellular communities called biofilms. Biofilms also form in the course of many infections. *Pseudomonas aeruginosa* infections frequently involve biofilms, which contribute materially to the difficulty to treat these infections with antibiotic therapy. Many biofilm-related characteristics are controlled by the second messenger, cyclic-di-GMP, which is upregulated on surface contact. Among these factors is the exopolysaccharide Psl, which is a critically important component of the biofilm matrix. Here we describe the discovery of a *P. aeruginosa* bacteriophage, which we have called Clew-1, that directly binds to and uses Psl as a receptor. While this phage does not efficiently infect planktonically growing bacteria, it can disrupt *P. aeruginosa* biofilms and replicate in biofilm bacteria. We further demonstrate that the Clew-1 can reduce the bacterial burden in a mouse model of *P. aeruginosa* keratitis, which is characterized by the formation of a biofilm on the cornea. Due to its reliance on Psl for infection, Clew-1 does not actually form plaques on wild-type bacteria under standard *in vitro* conditions. This argues that our standard isolation procedures likely exclude bacteriophage that are adapted to using biofilm markers for infection. Importantly, the manner in which we isolated Clew-1 can be easily extended to other strains of *P. aeruginosa* and indeed other bacterial species, which will fuel the discovery of other biofilm-tropic bacteriophage and expand their therapeutic use.

42 **Introduction**

43 Biofilms formed by bacteria at sites of infection significantly increase the difficulty of treatment
44 with conventional antibiotic therapy. This increased resistance to antibiotic therapy has been attributed
45 to a variety of factors, including reduced penetration of antibiotics (1, 2), as well as an increase in
46 antibiotic-tolerant persister bacteria (3, 4). Formation of biofilms is a feature of many *P. aeruginosa*
47 infections, including lung infections in cystic fibrosis patients (5, 6), wound, catheter, and device infections
48 (7), as well as blinding corneal infections (8-10). In some instances, these biofilms have been found to
49 be astonishingly antibiotic tolerant (11).

50 In addition to the antibiotic tolerance of bacteria in biofilms, there has been a significant increase
51 in antibiotic resistant isolates (12). In fact, *P. aeruginosa* is one of the particularly worrisome ESKAPE
52 group of pathogens (13). With the general rise of antibiotic-resistant isolates, phage therapy has garnered
53 some interest as an alternative to treat these infections (14, 15). However, biofilm formation frequently
54 interferes with phage infection (16), and even though a few bacteriophage that can target *P. aeruginosa*
55 in a biofilm have been described (17, 18), the mechanism by which they infect these biofilm bacteria is
56 unknown.

57 The extracellular matrix of *P. aeruginosa* biofilms is comprised of exopolysaccharides, including
58 Psl, Pel, and alginate, as well as proteins and DNA (19, 20). Psl is of significant interest, since it is critical
59 for biofilm formation, where it is needed for the initial surface attachment (21), as well as structural stability
60 of the mature biofilm (22). Psl has been detected on the surface of individual *P. aeruginosa* bacteria in
61 an apparent helical pattern (20). It is also deposited on surfaces by a subset of motile explorer bacteria
62 during the early stages of aggregate formation (23). Psl production interferes with complement deposition
63 and neutrophil functions, such as phagocytosis and ROS production (24). Moreover, Psl enhances the
64 intracellular survival of phagocytosed *P. aeruginosa*, as well as survival in mouse models of lung and
65 wound infection (24).

66 Here we describe the discovery of a bacteriophage that uses Psl, this crucial biofilm
67 exopolysaccharide, as a receptor. Interestingly, this bacteriophage only infects a subpopulation of
68 planktonically growing *P.* aeruginosa, but it can disrupt biofilms and replicates efficiently on biofilm-grown

69 bacteria. Moreover, the phage can reduce the bacterial burden in a corneal infection model, which
70 involves formation of a biofilm.
71
72 **Results**
73 **Phage Clew-1 can form plaques on a Δ*fliF* mutant, but not wild type *P. aeruginosa*.**
74 We screened wastewater samples at the three Northeast Ohio Regional Sewer District water
75 treatment plants in Cleveland for bacteriophage. The majority of phage in these samples used type IV
76 pili as a receptor, and we wanted to exclude these from our screen. We had previously generated a Δ*fliF*
77 Δ*pilA* double mutant strain in the lab and decided to use it to exclude both surface appendages as
78 potential receptors. This turned out to be fortuitous, since, surprisingly, the screen identified four phage
79 that could form plaques on the Δ*fliF* Δ*pilA* double mutant strain, but not the parental wild type *P.*
80 *aeruginosa* PAO1. We named these Cleveland wastewater-derived phage Clew-1, -3, -6, and -10.
81 Subsequent tests determined that it was the *fliF* deletion that rendered *P. aeruginosa* permissive for
82 infection by these phages. All four Clew phage can plaque on a *fliF* deletion mutant of *P. aeruginosa*
83 PAO1, but not the corresponding wild-type strain or Δ*pilA* mutant strain. (Fig. 1A, S1A, S1B, S2). An
84 unrelated Pbunavirus we isolated in the same screen, which uses O-antigen as receptor (Fig. S3), was
85 used as a control in these experiments (Our control phage, Ocp-2). The Clew bacteriophages belong to
86 the family of Bruynogheviruses (25) and are all highly related (Fig. 1B, S1C). Morphologically, like other
87 members of the family, they are Podoviruses (Fig. 1C).
88
89 **c-di-GMP levels control infection of *P. aeruginosa* by bacteriophage Clew-1.**
90 We next examined what part of the flagellum is involved in determining sensitivity to the Clew-1
91 phage. Mutations affecting the MS-ring (Δ*fliF*) and associated proteins FliE or FliG (26) resulted in Clew-
92 1 sensitivity. However, mutations in the ATPase complex only conferred partial sensitivity, and mutations
93 affecting the hook or flagellar filament did not result in sensitivity, nor did a mutation that affects the type
94 III secretion function of the flagellar basal body by impeding proton flux, *flhA(R147A)*(27), (Fig.S4). We
95 therefore conclude that it is the presence of the MS-ring and not other aspects of the flagellum, such as
96 assembly of the full flagellar structure or flagellar rotation, that control phage sensitivity.

97 Interestingly, we found that deletion of *fleQ*, which is required for transcription of flagellar genes
98 (28), had a very minor effect on Clew-1 phage susceptibility of the wild-type bacteria, and actually
99 decreased Clew-1 susceptibility of the Δ*fliF* mutant bacteria (Fig. S1E). FleQ is a c-di-GMP-responsive
100 transcription factor that, among other things, reciprocally controls flagellar gene expression and
101 production of biofilm-related characteristics, such as the production of the extracellular polysaccharides
102 Psl and Pel, as well as the adhesin CdrA (28-30). We therefore examined whether manipulating c-di-
103 GMP levels controls phage susceptibility. To this end we produced the c-di-GMP phosphodiesterase
104 PA2133 from a plasmid (31) to artificially lower c-di-GMP levels in the Δ*fliF2* deletion mutant strain.
105 Conversely, we artificially elevated c-di-GMP levels in the wild-type by deleting the *wspF* gene (31).
106 Lowering c-di-GMP levels in the Δ*fliF2* mutant restored Clew-1 resistance (Fig. 1D), whereas deleting
107 *wspF* rendered the parental PAO1 strain phage sensitive (Fig. 1E). Taken together, these data
108 demonstrate that Clew-1 susceptibility is controlled by intracellular c-di-GMP levels and argue that
109 absence of the MS-ring controls phage susceptibility through an increase in c-di-GMP.
110
111 **Phage Clew-1 requires Psl for infection.**
112 To better understand the host factors that control susceptibility and resistance to Clew-1 infection,
113 we carried out a pair of TnSeq experiments. In the first of these, we mutagenized the wild-type strain
114 PAO1F with the mini-mariner transposon TnFAC (32), and the resultant mutant library was infected with
115 phage Clew-1 at an MOI of 10 for 2 hours. The surviving bacteria were allowed to grow up after plating
116 on an LB plate and the transposon insertion sites for the input and output pool were determined by
117 Illumina sequencing. We identified insertion mutants that were depleted after infection (Fig. 2A). Two of
118 the genes with the most significant depletion were *fliF* and *fliG*, consistent with our previous analysis
119 indicating that these mutations sensitize PAO1 to Clew-1 infection. Interestingly we also noted depletion
120 of *pch* and *bifA* insertions, both encoding phosphodiesterases that are involved in depleting c-di-GMP in
121 the flagellated daughter cell after cell division (33-36). In fact, *pch* interacts with the chemotactic
122 machinery (33), highlighting, here too, the importance of c-di-GMP in controlling Clew-1 sensitivity.
123 In a reciprocal experiment, we carried out the TnSeq analysis in a *fliF* mutant strain. This analysis
124 identified insertions in the *psl* operon as the most highly enriched group of mutants after Clew-1 selection,

125 suggesting that Psl is required for phage infection (Fig. 2B). We examined the requirement for Psl
126 explicitly by generating *pslC* and *pslD* mutants in the PAO1F Δ*fliF2* strain background. PslC is a
127 glycosyltransferase required for Psl biosynthesis, while PslD is required for Psl export from the cell (37,
128 38). Deletion of either *pslC* or *pslD* rendered the *fliF* mutant bacteria Clew-1 resistant and sensitivity could
129 be restored through complementation using a plasmid-borne copy of the deleted open reading frame
130 (Fig. 2C). These data demonstrate that Psl production is required for infection of *P. aeruginosa* by phage
131 Clew-1.
132
133 **Phage Clew-1 attachment is Psl-dependent**
134 We next examined whether attachment of Clew-1 to *P. aeruginosa* is Psl-dependent. We first used
135 efficiency of center of infection (ECOI) analysis to examine attachment. In this analysis, the phage is
136 allowed to adhere to the bacteria for 5 minutes, before washing the bacteria to remove unattached phage.
137 The bacteria are then diluted, mixed with top agar and a sensitive indicator bacterium (Δ*fliF2*), and then
138 plated to allow for plaque formation as a biological readout of attached bacteriophage. Attachment of
139 phage Clew-1 is Psl-dependent. Interestingly, we were able to detect Psl-dependent attachment both
140 with wild-type and Δ*fliF2* mutant bacteria (Fig. 3A), which contradicted out initial efficiency of plating
141 experiments. We therefore reexamined phage susceptibility by monitoring phage infection in liquid media
142 and generating lysis curves for wild-type and Δ*fliF2* mutant bacteria, as well as their Δ*pslC* mutant
143 derivatives (Fig. S5). The Δ*fliF2* mutant strain was lysed after ~40 minutes of infection. The wild-type
144 bacteria displayed a significant slowing of growth upon Clew-1 infection when compared to the uninfected
145 culture, but not clear lysis as was observed with the Δ*fliF2* mutant. In both instances, deleting *pslC*
146 abolished any phage-dependent effect on growth.
147 We hypothesized that perhaps, the difference between wild-type and Δ*fliF2* mutant bacteria is due
148 to the fraction of cells that are producing Psl and therefore permissive for phage attachment. To test this
149 hypothesis, we labeled phage Clew-1 with the DyLight594 fluorescent dye and examined attachment
150 directly by microscopy (Fig. 3B). We observed a statistically significant increase in the percentage of
151 bacteria with attached bacteriophage in the Δ*fliF2* mutant bacteria compared to the wild-type, arguing
152 that the increase in c-di-GMP in the Δ*fliF2* mutant increases the fraction of Clew-1 susceptible cells in the

153 population. As anticipated, no phage was observed attached to the corresponding Δ*pslC* mutant (Fig.
154 3C).
155
156 **Phage Clew-1 binds to Psl directly**
157 We next examined whether phage Clew-1 can bind to Psl directly. We first determined whether
158 we could precipitate phage Clew-1 from filter sterilized culture supernatants of a Δ*fliF2* mutant using an
159 antibody directed against Psl. The presence of the phage was determined by quantitative PCR. We were
160 able to pull down phage Clew-1 in a Psl and antibody-dependent manner with Δ*fliF2* Δ*pslC* culture
161 supernatants serving as a control (Fig. 4A). Notably, we observed some Psl-dependent attachment in the
162 absence of antibody, arguing that Psl binds non-specifically to the magnetic beads we used in our
163 experiments. Including the anti-Psl antibody resulted in a statistically significant increase compared to
164 this background level of attachment (Fig. 4A). We next repeated the pulldown using a partially purified
165 fraction of cell-associated Psl to repeat the pulldown and again found Psl and antibody dependent
166 precipitation of phage Clew-1 (Fig. S7). Finally, we examined phage binding using a biotinylated, affinity
167 purified preparation of Psl and found that we could pull down the phage using this Psl fraction as well,
168 arguing that Clew-1 binds Psl directly (Fig. 4B).
169
170 **Phage Clew-1 infects wild-type *P. aeruginosa* in biofilms**
171 Since Clew-1 exploits Psl for infection and Psl is a key component of the biofilm matrix of most
172 strains of *P. aeruginosa* (39, 40), we hypothesized that, perhaps, Clew-1 can infect biofilm bacteria. We
173 used a static-biofilm model to test this hypothesis. Biofilms were established overnight in a 96-well plate.
174 One plate was washed and fixed with ethanol to quantify the day one biofilm mass using crystal violet
175 staining. In a second plate, established in parallel, the biofilms were washed with PBS and LB was added
176 back, either without addition, or with 10^9 pfu of phage Clew-1 or phage Ocp-2. The plates were
177 incubated overnight and the next day, the day 2 biofilm mass was quantified using crystal violet. A similar
178 experiment was carried out in 5-mL culture tubes to illustrate the result is shown in Fig. 5A. The averages
179 of 5 biological replicates in the 96-well experiment are shown in Fig. 5B. Treatment of the day one biofilm
180 with phage Clew-1 resulted in a statistically significant decrease in biofilm mass compared to the biomass

181 present at day 1. Phage Ocp-2 infection, on the other hand, did not result in a reduction in biofilm (Fig.
182 5B). Notably, phage Clew-1 was not able to reduce a biofilm formed by *P.* aeruginosa strain PA14, a
183 natural *psl* mutant (Fig. S8).

184 To corroborate this result, we also conducted a converse experiment where we monitored the
185 ability of phage Clew-1 or Ocp-2 to replicate on biofilm bacteria over a two-hour period. Here, biofilms
186 were generated overnight in 5-mL culture tubes, the biofilms were washed with PBS and exposed to 10^5
187 pfu/mL phage Clew-1 or phage Ocp-2 for 2 hours. At the end of the experiment, the culture supernatants
188 were filter sterilized and the phage were titered. Consistent with the reduction in biofilm mass seen in Fig.
189 5B, we found that phage Clew-1, but not Ocp-2, was able to replicate when grown on biofilm bacteria
190 (Fig. 5C).

191 In order to determine distinguish whether Clew-1 infection results in decolonization of bacteria
192 from the biofilm, or killing of biofilm bacteria, we carried out two complementary experiments. In the first
193 experiment, we generated wild type *P. aeruginosa* biofilms on polystyrene microbeads grown overnight
194 with agitation. The beads were then washed with PBS and incubated for 2 hours either in LB or LB with
195 Clew-1. Bacteria were released from the biofilm by sonication and the input CFU (total CFU attached to
196 beads) were compared to the output after 2h of incubation (sum of supernatant and bead-associated
197 viable bacteria). Clew-1 resulted in a significant reduction in viable CFU, arguing that phage infection kills
198 biofilm bacteria (Fig. 5D). In a related experiment, we used LIVE/DEAD staining of bacteria to assess
199 bacterial viability by microscopy. We established biofilms in microwell slides overnight, then added Syto
200 9 and propidium iodide (PI) to each well along with phage Clew-1, or a buffer control, and incubated the
201 slide overnight again before imaging the biofilms by confocal microscopy. Infection with Clew-1 resulted
202 in a significant increase in the fraction of the biofilm volume that is PI-positive, indicating that the biofilm
203 bacteria are dying (Fig. 5E).

204

205 **Phage Clew-1 can clear *P. aeruginosa* in a mouse keratitis model**

206 Given the ability of phage Clew-1 to infect *P. aeruginosa* biofilms, we next examined whether
207 Clew-1 could be used to treat a *P. aeruginosa* infection. Corneal infections by *P. aeruginosa* involve
208 formation of a biofilm (8, 40). In fact, a bivalent antibody directed against Psl and the type III secretion

209 needle-tip protein, PcrV, was found to be effective in clearing such corneal infections (8). We therefore
210 examined the ability of Clew-1 to reduce the *P. aeruginosa* bacterial burden in a corneal infection model.
211 Mice were infected with 5*10^4 cfu of wild-type *P. aeruginosa* strain PAO1 and given a topical application
212 of 5*10^9 pfu Clew-1 in 5μL of PBS, or PBS alone, at 24h and 48h post-infection (Fig. 6A). After 48 hours
213 the infection we quantified corneal opacity, a measure that correlates with the infiltration of immune cells
214 (41-43), and GFP fluorescence (produced by the *P. aeruginosa* strain used in the infection) by image
215 analysis. We also assessed the bacterial burden (colony forming units). Mice infected with PAO1
216 developed severe corneal disease manifest as corneal opacification in the region of bacterial growth
217 indicated by GFP fluorescence (Figure 6B-D). Phage Clew-1 treatment was able to significantly reduce
218 the bacterial burden, and in some instances completely eradicate the infection, as measured by GFP
219 fluorescence and CFU (Fig. 6D, E). Corneal opacity, was similarly reduced by the phage treatment,
220 indicating that inflammation was also starting to resolve (Fig. 6B, C).
221
222 **Summary**
223 We describe the isolation of four phage belonging to the family of Bruynogheviruses that use the
224 *P. aeruginosa* exopolysaccharide Psl as a receptor. Psl is not a capsular polysaccharide, so this
225 distinguishes the Clew phages from phages such as KP32 that infect *Klebsiella pneumoniae*. Moreover,
226 these *Klebsiella* phages use a capsular depolymerase to break down the capsular polysaccharide (44,
227 45). Clew-1, on the other hand, has no such activity (Fig. S9) arguing that the role of Psl in infection is
228 distinct from that seen in capsule-targeting bacteriophage.
229 Phage Clew-1 has the surprising quality that it fails to plaque on wild-type *P. aeruginosa* PAO1,
230 but forms plaques on a *fliF* mutant. We determined that the *fliF* mutation generates a c-di-GMP dependent
231 signal that up-regulates Psl production. Importantly, it increases the fraction of bacteria to which the
232 phage can bind, resulting in efficient lysis in liquid cultures, and plaque formation in top agar. Plaque
233 formation is likely masked in the wild-type bacteria by the fraction of cells that are not phage-susceptible.
234 Notably, certain Bruynogheviruses are able to bind to *P. aeruginosa* PAO1, but not plaque (46). We now
235 have an explanation for this observation.

236 The identification of Psl as phage receptor prompted us to examine the ability of phage Clew-1 to
237 infect wild-type *P. aeruginosa* in a biofilm. We found that phage Clew-1, unlike the unrelated Ocp-2 phage,
238 was able to disrupt biofilms formed by wild-type bacteria. Moreover, Clew-1 was able to actively replicate
239 on biofilm bacteria, while phage Ocp-2 could not. Taken together, our data suggests that phage Clew-1
240 has specialized to replicate on *P. aeruginosa* growing in a biofilm. Given the prevalence of bacterial
241 biofilms in nature, this specialization makes sense. Moreover, our observation suggests that we may
242 have underestimated the prevalence of biofilm-tropic bacteriophage since standard isolation techniques
243 using plaque formation of wild-type bacteria would miss phage akin to Clew-1. In fact, another
244 bacteriophage was recently described that requires an intact *psl* operon for replication and can only
245 plaque on PAO1 with elevated c-di-GMP levels (35). This bacteriophage, Knedl, belongs to the family of
246 Iggyvirueses (47), highlighting that more biofilm-tropic bacteriophage wait to be discovered. Our data
247 also suggest that, for *P. aeruginosa*, using a Δ*fliF* Δ*pilA* double mutant will allow us to enrich for biofilm-
248 specific bacteriophage, by excluding dominant type IV pilus-dependent phage and up-regulating biofilm-
249 specific surface structures such as Psl, Pel, and CdrA. Given the importance of biofilms in contributing to
250 the antibiotic resistance of *P. aeruginosa* in infections such as the CF lung, catheters or wound infections,
251 treatment modalities that are targeted towards biofilm bacteria are sorely needed. Indeed, phage Clew-
252 1 shows some promise in this regard, since it was able to kill biofilm bacteria *in vitro*, and control *P.*
253 aeruginosa infection in a mouse model of keratitis, which involves biofilm formation at the site of infection.
254 While Clew-1 plaques can sometimes look turbid, this is likely a function of the fact that Clew-1 can only
255 bind to a fraction of the bacterial population (80-90% in the case of PAO1 Δ*fliF2*, Fig. 3). We have not
256 been able to isolate Clew-1 lysogens, which is consistent with observations using other *Bruynogheviruses*
257 (18, 48, 49) and argues that Clew-1 is lytic and not temperate. While many bacteriophages are not able
258 to infect *P. aeruginosa* biofilms, some phage with the ability to target biofilms have been described,
259 including the *Bruynoghevirus* Delta (18). We present here a way by which phage that target *P. aeruginosa*
260 biofilms can be enriched during isolation.

261 Capsule-targeting bacteriophage tend to use LPS as a secondary receptor for tight binding to the
262 target cell. While Clew-1 does not seem to require either A- or B-band LPS for infection (Fig. S3), we did
263 hit several genes involved in the biosynthesis of outer core LPS in our TnSeq analysis (Table S3). We

264 tested whether one of these genes, *ssg* (PA5001), is required for Clew-1 infection and found that this is
265 the case (Fig. S3). How binding to Psl and LPS relate to the infection of *P. aeruginosa* by Clew-1 will be
266 examined in a future study.

267 Another interesting aspect of the work described herein is the relationship between the presence
268 of the MS-ring (FliF) and its associated proteins FliE and FliG with c-di-GMP levels. While it has been
269 noted previously that flagellar mutations lead to increases in c-di-GMP levels and increased production
270 of Psl upon surface contact (50), our results differ somewhat in that phage susceptibility was primarily
271 the result of loss of the MS-ring and associated proteins (FliEFG), not, for example, the flagellar filament
272 (FliC). This difference may be due to differences between planktonically grown (as in our study) and
273 surface-attached bacteria. Surface contact leads to up-regulation of c-di-GMP through surface sensing
274 by the Wsp chemosensory system (31, 51). Attached bacteria divide asymmetrically, with c-di-GMP levels
275 decreasing in the flagellated daughter cell (33-35, 52). This asymmetry requires the phosphodiesterase
276 Pch, which has been reported to bind to the chemosensory protein CheA (33, 34). A second
277 phosphodiesterase, BifA, is also required for maintaining c-di-GMP homeostasis and developing an
278 asymmetric program of cell division upon attachment to surfaces (35, 36). In our TnSeq experiment we
279 found that insertions in flagellar genes, such as *fliF* and *fliG*, but also insertions in *pch* and *bifA* resulted
280 in Clew-1 sensitivity. Whether the strong Clew-1 sensitivity associated with deletion of *fliF*, *fliE*, or *fliG* in
281 our data, relative to deletions in other flagellar components, relates to a pivotal role of the MS-ring in
282 controlling the activity of Pch and/or BifA is unclear, but worth further investigation. However, our work,
283 along with the work of the Jenal group (35), suggests that phage such as Clew-1 or Knedl could be a
284 useful tool for interrogating c-di-GMP signaling pathways in *P. aeruginosa*.

285 In summary, we have described here the isolation of a group of bacteriophages that target *P.*
286 *aeruginosa* biofilms by using the exopolysaccharide Psl as a receptor. Consistent with the critical role of
287 Psl as part of the *P. aeruginosa* biofilm matrix, we demonstrate that phage Clew-1 can replicate on biofilm
288 bacteria and control *P. aeruginosa* in a mouse model of keratitis. Moreover, we have described a
289 generalizable method that allows for the enrichment of biofilm-tropic bacteriophage, which is important
290 due to their potential utility in combating biofilm infections that are notoriously recalcitrant to antibiotic
291 therapy.

292 **Methods**

293 *Strain construction and culture conditions*

294 Bacterial strains were grown in LB (10g/L tryptone, 5g/L yeast extract, 5g/L NaCl) at 37°C unless
295 indicated otherwise. Bacterial strains and plasmids used in this study are listed in table S1. Mutations
296 were introduced into the genome of *P. aeruginosa* by allelic exchange. Briefly, flanks defining the mutation
297 were amplified from the *P. aeruginosa* genome and cloned into plasmid pEXG2 by Gibson cloning. The
298 primers used for the amplifications were designed using AmplifX 2.1.1 by Nicolas Jullien (Aix-Marseille
299 Univ, CNRS, INP, Inst Neurophysiopathol, Marseille, France - https://inp.univ-amu.fr/en/amplifx-manage-
300 test-and-design-your-primers-for-pcr) and are noted in table S2. Plasmid pEXG2 harboring the mutation
301 construct was transformed into *E. coli* strain SM10 and mated at 37°C into *P. aeruginosa* by mixing the
302 donor and recipient strains on an LB plate. The mating mixture was then plated on an LB plate with
303 30µg/mL gentamicin and 5µg/mL triclosan and grown overnight at 37°C (selecting against the *E. coli*
304 donor strain). Cointegrates were restruck and subsequently grown in LB lacking salt until the culture was
305 barely turbid. The bacteria were then plated on a sucrose plate (5% sucrose, 10g/L tryptone, 5g/L yeast
306 extract) and incubated overnight at 30°C. Sucrose resistant colonies were tested for gentamicin
307 sensitivity and the presence of the mutation was tested by PCR.

308 Complementing plasmids were generated by amplifying the open reading frame and using Gibson
309 assembly (53) to clone it into pPSV37. The plasmids were then transformed into *P. aeruginosa* by
310 electroporation.

311 For motility assays, individual bacterial colonies were used to inoculate motility agar plates (0.3%
312 agar, LB plates) and incubated at 37°C for ~8h before imaging the plate.

313

314 *Bacteriophage isolation and sequencing*

315 Bacteriophage were isolated from filter sterilized waste-water samples from one of three Northeast Ohio
316 Regional Sewer District wastewater treatment plants (Westerly, Southerly, or Easterly Sewage Treatment
317 plant). Phage were isolated by picking individual plaques isolated on *P. aeruginosa* PAO1 Δ*fliF* Δ*pilA* and
318 testing them for their ability to form plaques on the isolation strain or wild-type PAO1. Phage genome
319 DNA was isolated as previously described (54). Genomic DNA was sequenced by Illumina sequencing

320 and assembled using Spades version 3.15.3 (55). Genomes were annotated using PhageScope (56).
321 Genomes for Clew-1, Clew-3, Clew-6, and Clew-10, as well as Ocp-2, have been deposited in Genbank
322 [accession# PQ790658.1, PQ790659.1, PQ790660.1, PQ790661.1, and PQ790662.1].
323
324 *CsCl purification of bacteriophage*
325 Bacteriophage were purified by CsCl gradient based on a published protocol (57). Briefly, a 500mL culture
326 of PAO1F Δ*fliF2* was grown in LB to an OD_{600} of ~0.2 and inoculated with phage Clew-1 or Ocp-2 at an
327 MOI of 0.025. After about 4h of culture, the bacteria were pelleted (12,000 x g, 15 min, 4 ºC) and the
328 supernatant was filtered through a 0.2µM filter. The supernatant was treated with DNAse and RNAse
329 (1µg/mL each) overnight at 4°C. The following day, the phage were pelleted by centrifugation (overnight,
330 7,000 x g, 4 ºC), the supernatant discarded and the pellets were resuspended in 1mL of SM buffer (50mM
331 Tris.Cl (pH 7.5), 100mM NaCl, 8mM $MgSO_4$) without BSA each (~2h at 4°C). The concentrated phage
332 prep was then spun at 12,000xg for 10 minutes to pellet remaining cell debris. At this point, 0.75g of
333 CsCl/mL was added to the cleared supernatant and the mixture was spun for 20h at 4°C at 32000 rpm in
334 Beckman Optima MAX-TL ultracentrifuge using an MLS-50 rotor to establish the gradient. The band with
335 the phage was removed with a syringe and 20 gauge needle and transferred to a 3.5kDa cut-off dialysis
336 cassette (Slide-A-Lyzer, Thermo). The phage prep was dialyzed overnight against SM, then 2x for 3h
337 against SM, then overnight against PBS and 1x for 4h against PBS. The phage prep was tested for titer
338 and, in the case of Clew-1, the ability to plaque on a Δ*fliF2* mutant, but not wild-type PAO1F.
339
340 *Negative Stain Electron Microscopy*
341 The negative stain experiment was done as described previously (58). Briefly, a 3 µl phage Clew-
342 1 sample (0.1-0.5 mg/ml) was loaded onto glow-discharge carbon coated grid for 60 s at room
343 temperature and blotted with filter paper. The grid was touched with a water droplet and then blotted with
344 filter paper. This process was repeated twice. The grid was then touched with a drop of 0.75% uranyl
345 formate and blotted with filter paper. A second drop of 0.75% uranyl formate was applied to touch the grid
346 for 30 s, blotted with filter paper and then air dried before data collection. The images were taken by
347 Tecnai T20 (FEI Company) equipped with a Gatan 4K x 4K CCD camera at 80,000 x magnification.

348

349 *Efficiency of plating experiments*

350 To test phage plating efficiency, bacterial strains were back-diluted 1:200 from overnight cultures and
351 grown to early log phase (OD600 ~0.3). At this point, 50µL of culture were mixed with 3mL top agar (10g/L
352 tryptone, 5g/L yeast extract, 5g/L NaCl, 0.6% agar) and plated on an LB agar plate. Once solidified, 10-
353 fold serial dilutions of the phage in SMB buffer (50mM Tris.Cl (pH 7.5), 100mM NaCl, 8mM $MgSO_4$, 0.1%
354 bovine serum albumin). were spotted onto the agar using a multichannel pipette (3µL spots). The spots
355 were allowed to dry and the plates incubated overnight at 37°.

356

357 *Efficiency of Center of Infection (ECOI) experiments*

358 *P. aeruginosa* strains were grown to mid-logarithmic phase in LB supplemented with 5mM MgCl2
359 and 0.1mM MnCl2 (LBMM) concentrated and resuspended at a concentration of 10^9 cfu/mL in LBMM.
360 100µL bacterial suspensions were infected at an MOI of 1 with phage Clew-1 (2µL, 5*10^10 pfu/mL) for
361 5 mins at 37°C, then pelleted (3' 10k RPM), washed 2x with 1mL LB, and resuspended in 100µL LB. The
362 infected cells were serially diluted 10x, then 10µL of diluted, infected bacteria (10^-4 for WT and Δ*fliF2*;
363 10^-1 for Δ*pslC* and Δ*fliF2* Δ*pslC*) were mixed with 50µL of the mid-log PAO1F Δ*fliF2* culture and mixed
364 with 2.5mL top agar, plated on an LB plate and incubated overnight at 37·C. The following day, plaques
365 were counted to enumerate the cell-associated bacteria (59).

366

367 *TnSeq analysis*.

368 Strain PAO1F or PAO1F Δ*fliF* were mutagenized with transposon TnFac (32), a mini-mariner transposon
369 conferring gentamicin resistance. A pool 3*10^6 (PAO1F) or 6*10^6 (PAO1F Δ*fliF*) insertion mutants was
370 grown overnight, then diluted 1:200 in fresh LB and grown to an OD600 of 0.2. At this point the bacteria
371 were infected at an MOI of 10 with phage Clew-1 and incubated for 2h to allow infection and killing of
372 susceptible bacteria. Bacteria from 1mL culture were then pelleted, resuspended in 100µL LB with 5mM
373 EGTA, and plated on a 3 LB plates with 30µg/mL gentamicin. The next day, surviving bacteria that had
374 grown up where pooled and chromosomal DNA from the input and output pools were isolated using the
375 GenElute™ Bacterial Genomic DNA Kit (Millipore-Sigma). Library preparation followed a published

376 protocol (60). Genomic DNA was sheared to ~300bp using a Covaris focused ultrasonicator. The sheared
377 DNA was repaired using the NEBNext End Repair Module (New England Biolabs) and subsequently
378 tailed with a polly-dC tail using Terminal Transferase (New England Biolabs). Tailed chromosomal DNA
379 fragments were amplified in two consecutive steps, using primers Mar1x and olj376 for the first round
380 and Mar2-InSeq paired with a TdT_Index primer for the second round, based on the published protocol
381 (60). The libraries were sequenced using an Illumina MiniSeq system using the transposon-specific
382 primer MarSeq2. Reads with the correct Tn end sequence were mapped and tallied per site and per gene
383 using previously described scripts ((60) and https://github.com/lg9/Tn-seq). The data (hits and # of reads
384 for each gene) are listed for each strain and condition in Table S3.
385
386 *Clew-1 attachment by fluorescence microscopy*
387 Bacteriophage Clew-1 was isolated from 500mL of culture and purified using a CsCl gradient, following
388 a protocol published by the Center for Phage Technology at Texas A&M University. After dialysis overnight
389 dialysis of the phage into SM buffer, the phage was dialyzed 3 more times against PBS (2x for 3h and
390 once overnight). The purified phage was titered by efficiency of plating analysis and labeled with a
391 Dylight594 NHS-ester (Invigtrogen) at a concentration of 0.2mM, overnight in the dark. After labeling, the
392 residual dye was removed by gel filtration using a Performa DTR gel filtration cartridge (EdgeBio) that
393 had been equilibrated with PBS. The labeled phage preparation was titered to ensure that the phage
394 concentration was unchanged and that the phage had not lost infectivity.
395 To assess phage attachment, wild type PAO1F, PAO1F Δ*fliF2*, or PAO1F Δ*fliF2* Δ*pslC* harboring plasmid
396 pP25-GFPo, which directs the constitutive production of GFP, were grown in LB to an OD_{600} of ~0.3-0.4,
397 normalized to an OD_{600} of 03, and 0.5mL of the culture were infected for 10 minutes at 37°C with
398 DyLight594-labeled Clew-1 phage at an MOI of 5. At this point, the infected bacteria were fixed with 1.6%
399 paraformaldehyde [final concentration], incubated in the dark for 10 minutes, then the remaining
400 paraformaldehyde was quenched through the addition of 200μL of 1M glycine (10 minutes at RT). The
401 bacteria were washed 3x with 500μL of SM buffer and resuspended in 30μL SM buffer. 4μL were spotted
402 onto an agarose pad, covered with a coverslip and imaged using a Nikon Eclipse 90i fluorescence

403 microscope. Images were adjusted for contrast and false-colored using the Acorn software package
404 (Flying Meat Software), and cell-associated bacteriophage were counted in ImageJ.
405
406 *Isolation and purification of Psl polysaccharide*
407 Wild-type *P. aeruginosa* was grown for 18h in M63 minimal medium ($[NH_4]_2SO_4$, 2 g/l; KH_2PO_4, 13.6 g/l;
408 $FeCl_3$, 0.5 mg/l, pH 7) supplemented with 0.5% Casamino acids (BD), 1 mM $MgCl_2$, and 0.2% glucose.
409 Bacterial cells were removed by centrifugation, the supernatant lyophilized, and Psl isolated by affinity
410 chromatography.
411 The affinity column was prepared by resuspending 0.286 g of CNBr activated Sepharose
412 (Purchased from GE Healthcare; cat#17-0430-01) in 1 M HCl (1 mL). It was subsequently filtered and
413 washed with 1 M HCl (60 mL) and coupling buffer (1.5 mL; 0.1 M NaHCO3, 0.5 M NaCl, pH = 9). The
414 activated Sepharose was added to a solution of Cam-003 (61) in coupling buffer (0.5 mL; 10 mg/mL) and
415 was incubated for two hours at room temperature. The solvent was then removed by filtration, and the
416 beads were washed with coupling buffer (3 × 1 mL). After removal of the solvent the sepharose was
417 incubated with blocking buffer (2 mL; 0.1 M Tris, 0.5 M NaCl, pH = 8.5) for 2h at ambient temperature.
418 The beads were washed with wash buffer (4 mL) and coupling buffer (4 mL) for four cycles until the
419 OD280 of the wash was <0.01. The derivatized beads were loaded onto a column and after washing with
420 5 column volumes of PBS-buffer (pH=7.4) the affinity column was ready to use.
421 Crude Psl (100 mg) was dialyzed (Thermo Scientific SnakeSkinTM Dialysis Tubing 3K MWCO)
422 for three days and six exchanges of water and then concentrated to a final volume of 1 mL (10 mg/mL).
423 It was loaded onto the affinity column and washed with PBS-buffer (4 mL) in order to remove all not-
424 retained material. Next, the captured Psl was eluted with glycine buffer (4 mL; 100 mM glycine × HCl,
425 pH=2.7). The glycine fraction was dialyzed (3K MWCO) for three days and six exchanges of water and
426 after lyophilization, pure Psl (80 µg) was obtained.
427 The solution was lyophilized, and the residue was fractionated by gel permeation chromatography
428 on a Bio-Gel P-2 column (90 × 1.5 cm), eluted with 10 mM NH_4HCO_3. The collected fractions contained
429 different size of Psl material: dimer (two repeating units), trimer (three repeating units) and high molecular
430 weight polysaccharide. The high molecular weight polysaccharide fraction was used in our experiments.

431 Matrix-Assisted Laser Desorption/Ionization Time-of-Flight Mass Spectrometry experiments were
432 performed using Bruker ultrafleXtreme (Bruker Daltonics) mass spectrometer. All spectra were recorded
433 in reflector positive-ion mode and the acquisition mass range was 200–6000 Da. Samples were prepared
434 by mixing on the target 0.5 µL sample solutions with 0.5 µL aqueous 10% 2,5-dihydroxybenzoic acid as
435 matrix solution.
436
437 *Precipitation of Clew-1 from culture supernatants and using purified Psl*
438 For experiments in which binding of Clew-1 to Psl in culture supernatants was tested, PAO1F
439 Δ*fliF2* or PAO1F Δ*fliF2* Δ*pslC* were grown to mid-logarithmic phase, then the bacteria were pelleted and
440 the supernatants filter sterilized using a 0.2µM filter. Culture supernatants were mixed with 1µL of a rabbit,
441 anti-Psl antibody (37) as well as 10^7 pfu of phage Clew-1. The mixture was incubated on ice for 1h, then
442 10µL of magnetic protein A beads (BioRad), washed 2x with SMB + 0.05% Triton X-100 (SMBT) were
443 added to the mixture and incubated for an additional 30 minutes on ice. The magnetic beads were
444 collected, washed 3x with SMBT and resuspended in 100µl of SMBT. Presence of Clew-1 in input and
445 output samples was determined by quantitative PCR using primers designed to amplify the tail fiber gene,
446 gp12.
447 Experiments using partially purified, cell-associated Psl were carried out in SM buffer. 100µL of
448 SM-buffer were mixed with 10^7 pfu of phage Clew-1, as well as 1µg of a partially purified, deproteinated
449 fraction of cell-associated Psl (62) and incubated for 1h on ice. All subsequent steps were the same as
450 for the culture supernatants, above. Samples were resuspended in 100µL SMBT before quantifying Clew-
451 1 levels.
452 Experiments using affinity purified, biotinylated Psl were carried out in SM. Here too, 10^7 pfu
453 Clew-1 were incubated with 1µg of affinity purified, biotinylated Psl. The samples were either incubated
454 with streptavidin-coated Dynabeads (M280, Invitrogen) to precipitate the biotinylated Psl (or with
455 magnetic protein A beads as a specificity control). Otherwise, the experiments were carried out as for the
456 partially purified, cell-associated Psl fraction, above.
457
458 *Static biofilm experiments*

459 Static biofilm experiments were carried out based on a published protocol (63). *P. aeruginosa* PAO1F
460 was grown to mid-logarithmic phase in LB and then diluted to an OD600 of 0.05 and used to inoculate
461 either 5mL polystyrene tubes (1mL) or 6 wells in a polystyrene 96-well plate (150µL). The cultures were
462 incubated overnight at 37°C in a humidified incubator with a 5% CO2 atmosphere. The following day, 1
463 set of biofilm samples was washed three times with PBS, for 20 minutes fixed with 95% ethanol, and
464 subsequently air dried after removing the ethanol. The remaining biofilm samples were washed 2x with
465 PBS and reconstituted with pre-warmed LB (1.2mL in 5mL tube biofilms, 200µL. in 96-well plates), or LB
466 harboring either 10^9 pfu of phage Clew-1 or phage Ocp-2. The biofilm samples were again incubated
467 overnight at 37°C in a humidified incubator with a 5% CO2 atmosphere, and subsequently washed and
468 fixed as the control samples, above. The fixed and dried biofilms were stained with a 0.1% solution of
469 crystal violet in water for 30 minutes, the staining solution was removed, and the biofilms were washed
470 2x with mili-Q water and rinsed twice with deionized water before drying the stained biofilm samples. The
471 stained biofilms in the 5mL tubes were photographed against a white background. The stained biofilms
472 in the 96-well plates were incubated for 20 minutes in 200µL 30% acetic acid to solubilize the crystal
473 violet stain, which was subsequently quantified by spectrophotometry (absorbance at 590nm).
474
475 *Bead biofilm assay*
476 For each technical replicate (3 per condition), one 6mm natural bead (Precision Plastic Ball Company)
477 was placed in the well of a 24-well plate, and covered with 1mL of PAO1F in LB at an OD600 of 0.05.
478 The plate was sealed with parafilm and shaken overnight (150 rpm, 37°C). The following day all beads
479 were washed by moving the bead to 1mL sterile PBS with a forceps. Three beads were placed individually
480 into microcentrifuge tubes with 1mL PBS with 5mM $MgCl_2$, sonicated for 10 minutes in a water bath
481 sonicator, and titered on LB plates to determine the input. The remaining beads were transferred into
482 fresh wells of the 24-well plate with either 1mL LB or 1mL LB with 10^9 pfu Clew-1 and incubated with
483 shaking (37°C, 150rpm) for another 2 hours. At this point, the supernatant bacteria were titered, the beads
484 were washed 1x with PBS and placed individually into microcentrifuge tubes with 1mL PBS with 5mM
485 $MgCl_2$ and sonicated and titered, as above. The bacterial titers of the supernatant and bead-associated
486 bacteria were added to obtain the total CFU in the well and compared to the input CFU (bead titer at T0).

487 In some experiments, the phage treated samples were treated with a virucide before tittering (64). Here
488 250µL of 15% wt/vol, filter-sterilized black Tea was mixed with 730µL Milli-Q H2O and mixed with 20µL
489 of a freshly made, 200mM $FeSO_4$ solution just before use (4mM FeSO4 final). The virucide was mixed
490 with the sample, 1:1 and incubated for 10 minutes at room temperature before tittering the bacteria.
491 However, this did not significantly alter the outcome of the experiment, and the data presented are a
492 combination of all experiments, with and without virucide.
493
494 *LIVE/DEAD imaging of biofilms*
495 Biofilms were generated in 8-well chamber slides (ibidi) by inoculating the well with 200µL of mid-
496 log PAO1F (diluted to an OD_{600} 0.05) and incubating the slide overnight in a humidified incubator (5%
497 CO_2). The next day, the staining solution was added to each well (1µL of a 1:10 dilution of each
498 component in DMSO + 8µL LB) as well as 40 µL LB (no phage control) or 40µL LB with 10^9 pfu Clew-
499 1. The concentrations were based on a published protocol for using LIVE/DEAD staining to test antibiotic
500 susceptibility of biofilms (65).The slides were incubated overnight and imaged using a 60x objective on
501 a Nikon AX R laser scanning confocal microscope. The Z-stacks were analyzed and the propidium iodide
502 positive fraction of the total biofilm volume was determined using the BiofilmQ software package (66).
503
504 *Mouse keratitis model*
505 C57BL/6 mice were purchased from Jackson Laboratories. The mice were housed in pathogen free
506 conditions in microisolator cages and were treated according to institutional guidelines following approval
507 by the University of California IACUC.
508 Overnight cultures of P. aeruginosa PAO1F/pP25-GFPo were grown to log phase (OD_{600} of 0.2) in LB
509 broth, then washed and resuspended in PBS at $2.5x10^7$ bacteria/ml. 7-12 weeks old C57BL/6 mice were
510 anesthetized with ketamine/xylazine solution, the corneal epithelium was abraded with three parallel
511 scratches using a sterile 26-gauge needle, and 2 µL of a suspension of bacteria were added topically
512 (approximately $5x10^4$ cfu per eye). At 24h and 48h, the mice were anesthetized and treated with 5*10^9
513 pfu CsCl purified phage Clew-1 in PBS, or PBS alone. At 72h the mice were euthanized, and corneas
514 were imaged by brightfield microscopy to detect opacification, or by fluorescence microscopy to detect

515 GFP-expressing bacteria. Fluorescent intensity images were quantified using Image J software (NIH).
516 To determine the bacterial load, whole eyes were homogenized in PBS using a TissueLyser II (Qiagen,
517 30 Hz for 3 minutes), and homogenates were serially diluted plated on LB agar plates for quantification
518 of colony forming units (CFU) by manual counting. CFU were also determined at 2h to confirm the
519 inoculum.
520
521 *Growth curves*
522 Strains PAO1F, PAO1F Δ*fliF2*, PAO1F Δ*pslC*, and PAO1F Δ*fliF2* Δ*pslC* were grown to mid-logarithmic
523 phase in LB, then diluted to a concentration of 10^8 cfu/mL. For growth curve measurements (OD600),
524 3 technical replicates were set up in a 96-well plate for each strain/condition. 100µL of culture were mixed
525 with 10µL PBS or 10µL with 10^8 pfu Clew-1 and incubated at 37°C in an Agilent Cytation 5 Imaging
526 Plate Reader with a heated chamber and orbital rotation between OD600 measurements. OD600
527 readings were taken every 5 minutes.
528
529 *Culture Supernatant Psl blot*
530 Strains PAO1F Δ*fliF2* and PAO1F Δ*fliF2* Δ*pslC* were grown to mid-logarithmic phase (OD600 ~0.5), the
531 bacteria pelleted by centrifugation and the culture supernatant was sterilized using a 0.22µM syringe
532 filter. 0.5mL supernatant samples were incubated for 1h at 37°C with or without 10^7 pfu Clew-1 and
533 subsequently diluted three times at a 1:3 ratio. 2µL of the undiluted culture supernatants and of each
534 dilution were spotted onto a nitrocellulose filter and allowed to air-dry. The filter was then blocked with
535 5% non-fat milk in TBS-T (20mM Tris.Cl, 150mM NaCl, 0.1% Tween-20) for 30 minutes, washed 2x with
536 TBS-T and incubated with the primary anti-Psl antibody (diluted 1:3000) in TBS-T overnight at 4°C. The
537 following day, the blot was washed 3x with TBS-T, then incubated with secondary antibody (horse-radish
538 peroxidase conjugated goat anti-rabbit antibody, Sigma) diluted 1:10000 in TBS-T for ~3h at room
539 temperature. The blot was then washed 3x with TBS-T and developed using the Advansta WesternBright
540 Sirius HRP substrate and imaged on a GE ImageQuant LAS4000 imager.
541
542 *Analysis of Evolutionary Relatedness*

543 The evolutionary relationship between Clew bacteriophage and other Bruynogheviruses was carried out
544 using the Maximum Likelihood method and JTT matrix-based model (67). The tree with the highest log
545 likelihood is shown. Initial tree(s) for the heuristic search were obtained automatically by applying
546 Neighbor-Join and BioNJ algorithms to a matrix of pairwise distances estimated using the JTT model,
547 and then selecting the topology with superior log likelihood value. The tree is drawn to scale, with branch
548 lengths measured in the number of substitutions per site. This analysis involved 12 amino acid
549 sequences. There was a total of 485 positions in the final dataset. Evolutionary analyses were conducted
550 in MEGA11(68, 69). The genome comparison between Luz24 and the Clew phages was visualized using
551 EasyFig (70).
552
553

554 **Acknowledgements**

555 This work was made possible through an award by the Hypothesis fund. The authors would like to thank
556 the Northeast Ohio Regional Sewer District, and in particular Scott Broski and Leslie Vankuren, for
557 providing the wastewater samples from which the bacteriophage described in this study were isolated.
558 We wish to acknowledge Sabrina Lamont and Tony DiCesare (Wozniak lab) who provided Psl
559 preparations and αPsl rabbit polyclonal antibody for the studies described. The authors would like to
560 thank Dr. George Dubyak for the use of his spectrophotometer/plate reader. We would like to thank Dr.
561 Joseph Mougous for providing us with unpublished *pslC* and *pslD* complementation plasmids. We would
562 also like to thank Dr. Mougous and Dr. Simon Dove for their support and for critical reading of the
563 manuscript, and Dr. Matthew Parsek for his enthusiasm for the project and helpful discussions. This
564 manuscript was supported by NIH grant R01AI169865 (to D.J.W.), grant R01EY14362 (to E.P.), and grant
565 R01 AI145069 (to E.W.Y). The Psl-specific CAM003 antibody was obtained by G.-J.B. from AstraZeneca
566 (Dr. Antonio DiGiandomenico). The departmental Nikon AX R confocal microscope was supported by
567 1P30 DA054557 (to Alan Levine).

568

569 **Figure Legends**

570 **Fig. 1 c-di-GMP levels control infection of *P. aeruginosa* by bacteriophage Clew-1.** A) Efficiency
571 of plating experiment in which 3μL of a 10x dilution series of bacteriophage Ocp-2 or Clew-1 were
572 spotted on wild-type PAO1F, or PAO1F Δ*fliF2*. The adjacent graph shows the compiled results from 11
573 experiments. B) Maximum likelihood phylogenetic tree of Clew-1 relative to other Bruynogheviruses
574 (including the type phage, LUZ24) and phage Bjorn as an outgroup. Branch lengths are measured in
575 number of substitutions per site in the terminase large subunit. C) transmission electron micrograph of
576 the Clew-1 phage. D) Efficiency of plating experiment as in (A) assaying the effect of expressing the
577 phosphodiesterase PA2133 from a plasmid. E) Efficiency of plating experiment assaying the effect of
578 deleting *wspF* on Clew-1 resistance. (* $p<0.05$, **** $p<0.0001$ by Student's T-test (A, E) or 1-way
579 ANOVA with Šídák's multiple comparisons test (D))

580

581 **Fig. 2 Bacteriophage Clew-1 uses Psl as a receptor to infect *P. aeruginosa*.** A) TnSeq experiment
582 in which a pool of mariner transposon mutants of strain PAO1F were infected with phage Clew-1 for 2h.
583 The number of insertions in the output pool were plotted against the ratio of the output and input pool.
584 B) Similar TnSeq analysis as in A) but using PAO1F Δ*fliF2*. C) Efficiency of plating analysis on Δ*fliF2*
585 Δ*pslC* and Δ*fliF2* Δ*pslD,* Psl biosynthesis mutants, either harboring an empty vector or a complementing
586 plasmid (n=6). Clew-1 values were compared by 1-way ANOVA with Šídák's multiple comparisons test
587 (** $p<0.01$, n.s. .. not significant).

588

589 **Fig. 3. The Δ*fliF2* mutation changes the fraction of cells that phage Clew-1 binds to**. A) Efficiency
590 of center of infection analysis. The indicated strain was infected for 5 minutes at an MOI of 0.01, the
591 bacteria were pelleted, washed 3x with PBS, then diluted and mixed with an excess of the Δ*fliF2* mutant
592 strain, top agar and plated on an LB agar plate. The number of plaques was used to calculate the
593 number of phage that attached and productively infected the initial strain. B) Phage Clew-1 was labeled
594 with DyLight594 fluorophores, bound to the indicated wild-type or mutant bacteria (15 minutes in LB),
595 washed and fixed with paraformaldehyde. Phage attached to bacteria were imaged by fluorescence
596 microscopy and attachment was quantified over 5 biological replicates, shown in C). Attachment was

597 compared by 1-way ANOVA with Šídák's multiple comparisons test. * $p < 0.05$, *** $p<0.001$,****
598 $p<0.0001$.
599
600 **Fig. 4. Phage Clew-1 binds to Psl**. A) Sterile filtered mid-log culture supernatants of PAO1F Δ*fliF2* or
601 PAO1F Δ*fliF2* Δ*pslC* were incubated with phage Clew-1, as well as magnetic protein-A beads and,
602 where indicated, a rabbit, anti-Psl antiserum. Beads were collected, washed 3x, and phage in the input
603 and output samples were quantified by qPCR (7 independent replicates.) B) Phage Clew-1 was
604 incubated for 1h in SM buffer with affinity purified, biotinylated Psl (biotin-Psl) and magnetic protein A
605 beads, or magnetic streptavidin beads (SA), where indicated. Beads were collected and washed 3x,
606 and phage in the input and output samples were quantified by qPCR (3 independent replicates).
607 Statistical significance was determined by ANOVA with Sidák post-hoc test (**** $p<0.0001$).
608
609 **Fig. 5. Phage Clew-1 can infect *P. aeruginosa* in biofilms.** A) Biofilms of wild type *P.* aeruginosa
610 PAO1F were established overnight in 5mL culture tubes (1mL culture), the tubes were washed with
611 PBS and 1.2mL LB, LB with 10^10 pfu phage Clew-1, or LB-with 10^10 pfu phage Ocp-2 were added
612 back to each tube (1 was fixed with EtOH to represent the 1-day old biofilm). The following day all
613 biofilms were washed with PBS and stained with crystal violet. B) PAO1F biofilms were established
614 overnight in a 96-well plate (150μL of culture, 6 technical replicates/condition), washed and incubated
615 overnight with 200μL of LB or LB with 10^9 pfu bacteriophage Clew-1 or Ocp-2. The biofilms were then
616 washed, fixed, and stained with crystal violet, which was then quantified spectrophotometrically. The
617 day 1 controls were set to 100% (5 biological replicates). C) Growth of phage Clew-1 or Ocp-2 was
618 assayed by establishing a static biofilm in 5 mL culture tubes overnight. The biofilms were washed with
619 PBS, then LB with 10^5 pfu/mL of phage Clew-1 or Ocp-2 was added back. Biofilms were incubated at
620 37°C for 2h 15 minutes, the culture supernatants were filter sterilized and input and output phage
621 concentrations were tittered (6 biological replicates). D) Wild-type PAO1 biofilms were grown overnight,
622 with agitation, on 6mm polystyrene beads. Biofilms were rinsed with PBS and incubated with LB or LB
623 with 10^9 pfu Clew-1 for 2h. The sum of bead-associated and supernatant CFU were titered at the 2h
624 mark and compared to the bead-associated biofilm input (T0) to assess total viable CFU (7 biological

625 replicates). E) Biofilms were grown overnight in 8-well slides, at which point the LIVE/DEAD stain dyes,
626 Syto 9 and propidium iodide were added, either on their own (mock) or in the presence of Clew-1. After
627 another 24h of incubation, biofilms were imaged by confocal microscopy. Maximum intensity projections
628 of the collected Z-stacks for one replicate are shown, along with YZ and XZ projections to the right and
629 bottom of the image, respectively. The fraction of the total biofilm volume in the image stack that is
630 propidium iodide positive was determined using BiofilmQ (3 biological replicates). Statistical
631 significance was determined by ANOVA with Šídák's multiple comparisons test, except for panel E),
632 where a two-tailed, unpaired T-test was applied (* $p<0.05$, ** $p<0.01$, *** $p<0.001$).
633
634 **Fig. 6. Phage Clew-1 reduces the bacterial burden in a mouse cornea model of infection.** A) Mice
635 corneas were scratched and infected with 5*10^4 cfu strain PAO1F/pP25-GFPo, which produces GFP
636 constitutively. Infected corneas were treated with 2*10^9 pfu phage Clew-1 or a PBS control at 24h and
637 48h post infection. B) At 72h post infection, the corneas were imaged by confocal microscopy to
638 estimate the opacity (driven largely by the infiltration of neutrophils) and GFP fluorescence (produced
639 by infecting *P. aeruginosa*). Representative images are shown in B). Opacity and GFP fluorescence
640 were quantified by image analysis and are graphed in C) and D), respectively. E) Eyes were also
641 homogenized and plated for CFU to determine the total bacterial burden at the end of the experiment.
642 Significance was determined by Mann-Whitney test (C, D) or ANOVA with Kruskal Wallis post-hoc test
643 (E) (** $p<0.01$, **** $p<0.0001$).
644

References

1. Wilton M, Charron-Mazenod L, Moore R, Lewenza S. Extracellular DNA Acidifies Biofilms and Induces Aminoglycoside Resistance in Pseudomonas aeruginosa. Antimicrob Agents Chemother. 2016;60(1):544-53.
2. Chiang WC, Nilsson M, Jensen PO, Hoiby N, Nielsen TE, Givskov M, et al. Extracellular DNA shields against aminoglycosides in Pseudomonas aeruginosa biofilms. Antimicrob Agents Chemother. 2013;57(5):2352-61.
3. Ciofu O, Moser C, Jensen PO, Hoiby N. Tolerance and resistance of microbial biofilms. Nat Rev Microbiol. 2022;20(10):621-35.
4. Lewis K. Multidrug tolerance of biofilms and persister cells. Curr Top Microbiol Immunol. 2008;322:107-31.
5. Hoiby N, Ciofu O, Bjarnsholt T. Pseudomonas aeruginosa biofilms in cystic fibrosis. Future Microbiol. 2010;5(11):1663-74.
6. Mulcahy LR, Burns JL, Lory S, Lewis K. Emergence of Pseudomonas aeruginosa strains producing high levels of persister cells in patients with cystic fibrosis. J Bacteriol. 2010;192(23):6191-9.
7. Ledizet M, Murray TS, Puttagunta S, Slade MD, Quagliarello VJ, Kazmierczak BI. The ability of virulence factor expression by Pseudomonas aeruginosa to predict clinical disease in hospitalized patients. PLoS One. 2012;7(11):e49578.
8. Thanabalasuriar A, Scott BNV, Peiseler M, Willson ME, Zeng Z, Warrener P, et al. Neutrophil Extracellular Traps Confine Pseudomonas aeruginosa Ocular Biofilms and Restrict Brain Invasion. Cell Host Microbe. 2019;25(4):526-36 e4.
9. Behlau I, Gilmore MS. Microbial biofilms in ophthalmology and infectious disease. Arch Ophthalmol. 2008;126(11):1572-81.
10. Okurowska K, Monk PN, Karunakaran E. Increased tolerance to commonly used antibiotics in a Pseudomonas aeruginosa ex vivo porcine keratitis model. Microbiology (Reading). 2024;170(5).
11. Hamed K, Debonnett L. Tobramycin inhalation powder for the treatment of pulmonary Pseudomonas aeruginosa infection in patients with cystic fibrosis: a review based on clinical evidence. Ther Adv Respir Dis. 2017;11(5):193-209.
12. D'Agata EM. Rapidly rising prevalence of nosocomial multidrug-resistant, Gram-negative bacilli: a 9-year surveillance study. Infect Control Hosp Epidemiol. 2004;25(10):842-6.
13. Rice LB. Federal funding for the study of antimicrobial resistance in nosocomial pathogens: no ESKAPE. J Infect Dis. 2008;197(8):1079-81.
14. Qin S, Xiao W, Zhou C, Pu Q, Deng X, Lan L, et al. Pseudomonas aeruginosa: pathogenesis, virulence factors, antibiotic resistance, interaction with host, technology advances and emerging therapeutics. Signal Transduct Target Ther. 2022;7(1):199.
15. Yin C, Alam MZ, Fallon JT, Huang W. Advances in Development of Novel Therapeutic Strategies against Multi-Drug Resistant Pseudomonas aeruginosa. Antibiotics. 2024;13(2):119.
16. Luthe T, Kever L, Thormann K, Frunzke J. Bacterial multicellular behavior in antiviral defense. Curr Opin Microbiol. 2023;74:102314.
17. Manohar P, Loh B, Turner D, Tamizhselvi R, Mathankumar M, Elangovan N, et al. In vitro and in vivo evaluation of the biofilm-degrading Pseudomonas phage Motto, as a candidate for phage therapy. Frontiers in microbiology. 2024;15:1344962.
18. Knezevic P, Petrovic Fabijan A, Gavric D, Pejic J, Doffkay Z, Rakhely G. Phages from Genus Bruynoghevirus and Phage Therapy: Pseudomonas Phage Delta Case. Viruses. 2021;13(10).
19. Ma LZ, Wang D, Liu Y, Zhang Z, Wozniak DJ. Regulation of Biofilm Exopolysaccharide Biosynthesis and Degradation in Pseudomonas aeruginosa. Annu Rev Microbiol. 2022;76:413-33.
20. Ma L, Conover M, Lu H, Parsek MR, Bayles K, Wozniak DJ. Assembly and development of the Pseudomonas aeruginosa biofilm matrix. PLoS Pathog. 2009;5(3):e1000354.
21. Byrd MS, Pang B, Mishra M, Swords WE, Wozniak DJ, Pier G. The Pseudomonas aeruginosa Exopolysaccharide Psl Facilitates Surface Adherence and NF-κB Activation in A549 Cells. mBio. 2010;1(3).
22. Colvin KM, Irie Y, Tart CS, Urbano R, Whitney JC, Ryder C, et al. The Pel and Psl polysaccharides provide Pseudomonas aeruginosa structural redundancy within the biofilm matrix. Environ Microbiol. 2012;14(8):1913-28.

23. Zhao K, Tseng BS, Beckerman B, Jin F, Gibiansky ML, Harrison JJ, et al. Psl trails guide exploration and microcolony formation in Pseudomonas aeruginosa biofilms. Nature. 2013;497(7449):388-91.
24. Mishra M, Byrd MS, Sergeant S, Azad AK, Parsek MR, McPhail L, et al. Pseudomonas aeruginosa Psl polysaccharide reduces neutrophil phagocytosis and the oxidative response by limiting complement-mediated opsonization. Cell Microbiol. 2012;14(1):95-106.
25. Lefkowitz EJ, Dempsey DM, Hendrickson RC, Orton RJ, Siddell SG, Smith DB. Virus taxonomy: the database of the International Committee on Taxonomy of Viruses (ICTV). Nucleic Acids Res. 2018;46(D1):D708-D17.
26. Minamino T, Kawamoto A, Kinoshita M, Namba K. Molecular Organization and Assembly of the Export Apparatus of Flagellar Type III Secretion Systems. Bacterial Type III Protein Secretion Systems. Current Topics in Microbiology and Immunology2019. p. 91-107.
27. Erhardt M, Wheatley P, Kim EA, Hirano T, Zhang Y, Sarkar MK, et al. Mechanism of type-III protein secretion: Regulation of FlhA conformation by a functionally critical charged-residue cluster. Mol Microbiol. 2017;104(2):234-49.
28. Arora SK, Ritchings BW, Almira EC, Lory S, Ramphal R. A transcriptional activator, FleQ, regulates mucin adhesion and flagellar gene expression in Pseudomonas aeruginosa in a cascade manner. J Bacteriol. 1997;179(17):5574-81.
29. Oladosu VI, Park S, Sauer K. Flip the switch: the role of FleQ in modulating the transition between the free-living and sessile mode of growth in Pseudomonas aeruginosa. J Bacteriol. 2024;206(3):e0036523.
30. Dasgupta N, Wolfgang MC, Goodman AL, Arora SK, Jyot J, Lory S, et al. A four-tiered transcriptional regulatory circuit controls flagellar biogenesis in Pseudomonas aeruginosa. Molecular Microbiology. 2003;50(3):809-24.
31. Hickman JW, Tifrea DF, Harwood CS. A chemosensory system that regulates biofilm formation through modulation of cyclic diguanylate levels. Proc Natl Acad Sci U S A. 2005;102(40):14422-7.
32. Wong SM, Mekalanos JJ. Genetic footprinting with mariner-based transposition in Pseudomonas aeruginosa. Proc Natl Acad Sci U S A. 2000;97(18):10191-6.
33. Kulasekara BR, Kamischke C, Kulasekara HD, Christen M, Wiggins PA, Miller SI. c-di-GMP heterogeneity is generated by the chemotaxis machinery to regulate flagellar motility. eLife. 2013;2.
34. Laventie B-J, Sangermani M, Estermann F, Manfredi P, Planes R, Hug I, et al. A Surface-Induced Asymmetric Program Promotes Tissue Colonization by Pseudomonas aeruginosa. Cell Host & Microbe. 2019;25(1):140-52.e6.
35. Manner C, Dias Teixeira R, Saha D, Kaczmarczyk A, Zemp R, Wyss F, et al. A genetic switch controls Pseudomonas aeruginosa surface colonization. Nat Microbiol. 2023;8(8):1520-33.
36. Kuchma SL, Brothers KM, Merritt JH, Liberati NT, Ausubel FM, O'Toole GA. BifA, a cyclic-Di-GMP phosphodiesterase, inversely regulates biofilm formation and swarming motility by Pseudomonas aeruginosa PA14. J Bacteriol. 2007;189(22):8165-78.
37. Byrd MS, Sadovskaya I, Vinogradov E, Lu H, Sprinkle AB, Richardson SH, et al. Genetic and biochemical analyses of the Pseudomonas aeruginosa Psl exopolysaccharide reveal overlapping roles for polysaccharide synthesis enzymes in Psl and LPS production. Molecular Microbiology. 2009;73(4):622-38.
38. Wu H, Wang D, Tang M, Ma LZ. The advance of assembly of exopolysaccharide Psl biosynthesis machinery in Pseudomonas aeruginosa. Microbiologyopen. 2019;8(10):e857.
39. Tabor DE, Oganesyan V, Keller AE, Yu L, McLaughlin RE, Song E, et al. Pseudomonas aeruginosa PcrV and Psl, the Molecular Targets of Bispecific Antibody MEDI3902, Are Conserved Among Diverse Global Clinical Isolates. J Infect Dis. 2018;218(12):1983-94.
40. Zegans ME, DiGiandomenico A, Ray K, Naimie A, Keller AE, Stover CK, et al. Association of Biofilm Formation, Psl Exopolysaccharide Expression, and Clinical Outcomes in Pseudomonas aeruginosa Keratitis: Analysis of Isolates in the Steroids for Corneal Ulcers Trial. JAMA ophthalmology. 2016;134(4):383-9.
41. Sun Y, Karmakar M, Roy S, Ramadan RT, Williams SR, Howell S, et al. TLR4 and TLR5 on corneal macrophages regulate Pseudomonas aeruginosa keratitis by signaling through MyD88-dependent and -independent pathways. J Immunol. 2010;185(7):4272-83.

42. Hazlett LD, Zucker M, Berk RS. Distribution and kinetics of the inflammatory cell response to ocular challenge with Pseudomonas aeruginosa in susceptible versus resistant mice. Ophthalmic Res. 1992;24(1):32-9.
43. Lee EJ, Cowell BA, Evans DJ, Fleiszig SM. Contribution of ExsA-regulated factors to corneal infection by cytotoxic and invasive Pseudomonas aeruginosa in a murine scarification model. Invest Ophthalmol Vis Sci. 2003;44(9):3892-8.
44. Squeglia F, Maciejewska B, Łątka A, Ruggiero A, Briers Y, Drulis-Kawa Z, et al. Structural and Functional Studies of a Klebsiella Phage Capsule Depolymerase Tailspike: Mechanistic Insights into Capsular Degradation. Structure. 2020;28(6):613-24.e4.
45. Dunstan RA, Bamert RS, Belousoff MJ, Short FL, Barlow CK, Pickard DJ, et al. Mechanistic Insights into the Capsule-Targeting Depolymerase from a Klebsiella pneumoniae Bacteriophage. Microbiology Spectrum. 2021;9(1).
46. Costa AR, van den Berg DF, Esser JQ, Muralidharan A, van den Bossche H, Bonilla BE, et al. Accumulation of defense systems in phage-resistant strains of Pseudomonas aeruginosa. Sci Adv. 2024;10(8):eadj0341.
47. Maffei E, Manner C, Jenal U, Harms A. Complete genome sequence of Pseudomonas aeruginosa phage Knedl. Microbiol Resour Announc. 2024;13(4):e0117423.
48. Ceyssens P-J, Hertveldt K, Ackermann H-W, Noben J-P, Demeke M, Volckaert G, et al. The intron-containing genome of the lytic Pseudomonas phage LUZ24 resembles the temperate phage PaP3. Virology. 2008;377(2):233-8.
49. Alvi IA, Asif M, Ur Rehman S. A single dose of a virulent bacteriophage vB PaeP-SaPL, rescues bacteremic mice infected with multi drug resistant Pseudomonas aeruginosa. Virus Res. 2021;292:198250.
50. Harrison JJ, Almblad H, Irie Y, Wolter DJ, Eggleston HC, Randall TE, et al. Elevated exopolysaccharide levels in Pseudomonas aeruginosa flagellar mutants have implications for biofilm growth and chronic infections. PLoS Genet. 2020;16(6):e1008848.
51. Armbruster CR, Lee CK, Parker-Gilham J, de Anda J, Xia A, Zhao K, et al. Heterogeneity in surface sensing suggests a division of labor in Pseudomonas aeruginosa populations. eLife. 2019;8.
52. Christen M, Kulasekara HD, Christen B, Kulasekara BR, Hoffman LR, Miller SI. Asymmetrical distribution of the second messenger c-di-GMP upon bacterial cell division. Science. 2010;328(5983):1295-7.
53. Gibson DG, Young L, Chuang RY, Venter JC, Hutchison CA, 3rd, Smith HO. Enzymatic assembly of DNA molecules up to several hundred kilobases. Nat Methods. 2009;6(5):343-5.
54. Jakociune D, Moodley A. A Rapid Bacteriophage DNA Extraction Method. Methods Protoc. 2018;1(3).
55. Prjibelski A, Antipov D, Meleshko D, Lapidus A, Korobeynikov A. Using SPAdes De Novo Assembler. Curr Protoc Bioinformatics. 2020;70(1):e102.
56. Wang RH, Yang S, Liu Z, Zhang Y, Wang X, Xu Z, et al. PhageScope: a well-annotated bacteriophage database with automatic analyses and visualizations. Nucleic Acids Res. 2024;52(D1):D756-D61.
57. Piya D, Vara L, Russell WK, Young R, Gill JJ. The multicomponent antirestriction system of phage P1 is linked to capsid morphogenesis. Mol Microbiol. 2017;105(3):399-412.
58. Booth DS, Avila-Sakar A, Cheng Y. Visualizing proteins and macromolecular complexes by negative stain EM: from grid preparation to image acquisition. J Vis Exp. 2011(58).
59. Hyman P, Abedon ST. Bacteriophage host range and bacterial resistance. Adv Appl Microbiol. 2010;70:217-48.
60. Gallagher LA. Methods for Tn-Seq Analysis in Acinetobacter baumannii. Methods Mol Biol. 2019;1946:115-34.
61. DiGiandomenico A, Warrener P, Hamilton M, Guillard S, Ravn P, Minter R, et al. Identification of broadly protective human antibodies to Pseudomonas aeruginosa exopolysaccharide Psl by phenotypic screening. J Exp Med. 2012;209(7):1273-87.
62. Chiba A, Sugimoto S, Sato F, Hori S, Mizunoe Y. A refined technique for extraction of extracellular matrices from bacterial biofilms and its applicability. Microb Biotechnol. 2015;8(3):392-403.
63. O'Toole GA. Microtiter dish biofilm formation assay. J Vis Exp. 2011(47).

807 64. Liu H, Meng R, Wang J, Niu YD, Li J, Stanford K, et al. Inactivation of Escherichia coli O157
808 Bacteriophages by Using a Mixture of Ferrous Sulfate and Tea Extract. J Food Prot. 2015;78(12):2220-
809 6.
810 65. Müsken M, Di Fiore S, Romling U, Häussler S. A 96-well-plate-based optical method for the
811 quantitative and qualitative evaluation of Pseudomonas aeruginosa biofilm formation and its application
812 to susceptibility testing. Nat Protoc. 2010;5(8):1460-9.
813 66. Hartmann R, Jeckel H, Jelli E, Singh PK, Vaidya S, Bayer M, et al. Quantitative image analysis of
814 microbial communities with BiofilmQ. Nat Microbiol. 2021;6(2):151-6.
815 67. Jones DT, Taylor WR, Thornton JM. The rapid generation of mutation data matrices from protein
816 sequences. Comput Appl Biosci. 1992;8(3):275-82.
817 68. Stecher G, Tamura K, Kumar S. Molecular Evolutionary Genetics Analysis (MEGA) for macOS.
818 Mol Biol Evol. 2020;37(4):1237-9.
819 69. Tamura K, Stecher G, Kumar S. MEGA11: Molecular Evolutionary Genetics Analysis Version 11.
820 Mol Biol Evol. 2021;38(7):3022-7.
821 70. Sullivan MJ, Petty NK, Beatson SA. Easyfig: a genome comparison visualizer. Bioinformatics.
822 2011;27(7):1009-10.
823

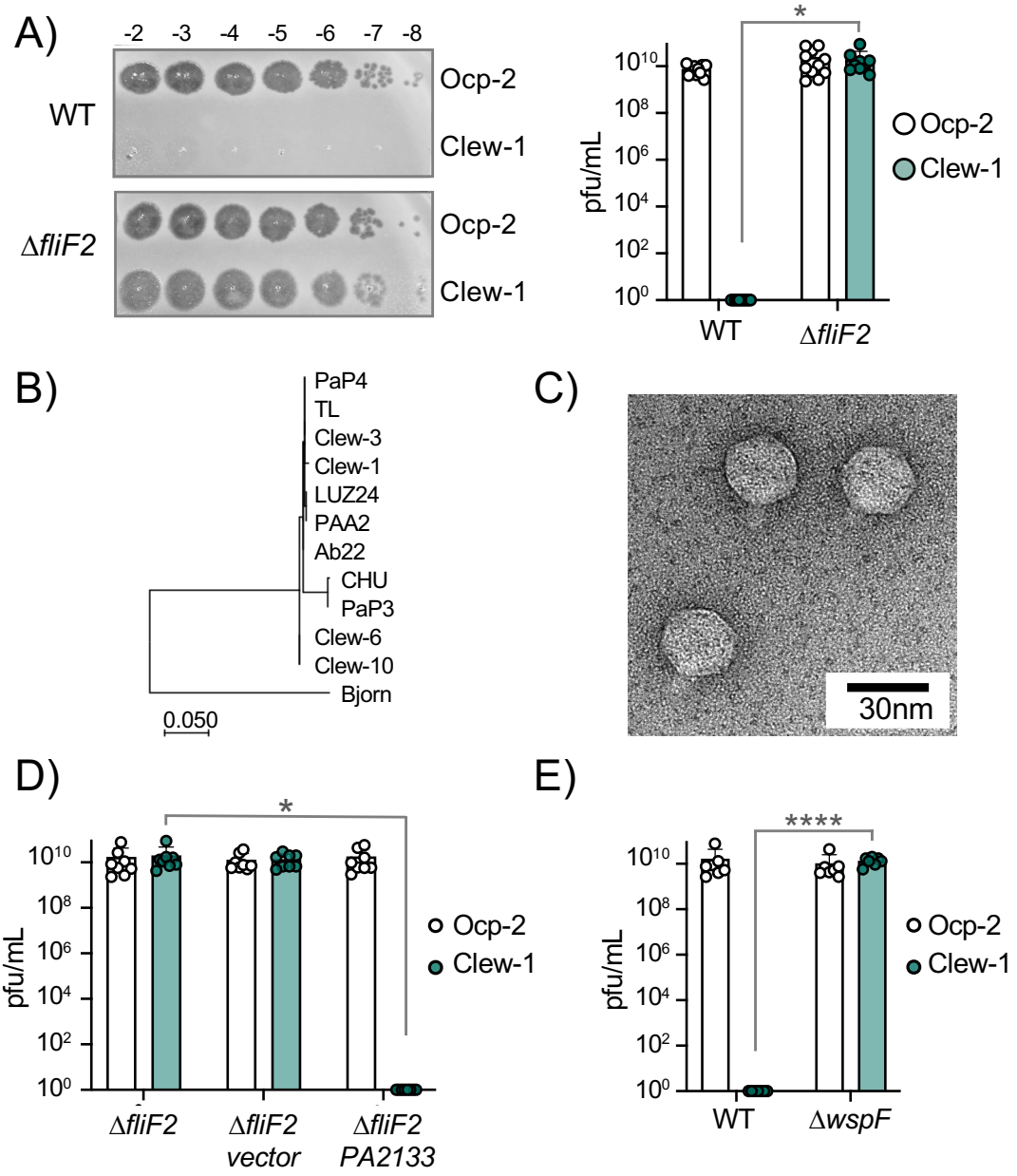
A)
-2 -3 -4 -5 -6 -7 -8
WT
Ocp-2
Clew-1
ΔfliF2
Ocp-2
Clew-1
*
pfu/mL
Ocp-2
Clew-1
WT
ΔfliF2
B)
PaP4
TL
Clew-3
Clew-1
LUZ24
PAA2
Ab22
CHU
PaP3
Clew-6
Clew-10
Bjorn
0.050
C)
30nm
D)
*
pfu/mL
Ocp-2
Clew-1
ΔfliF2
ΔfliF2 vector
ΔfliF2 PA2133
E)
****
pfu/mL
Ocp-2
Clew-1
WT
ΔwspF

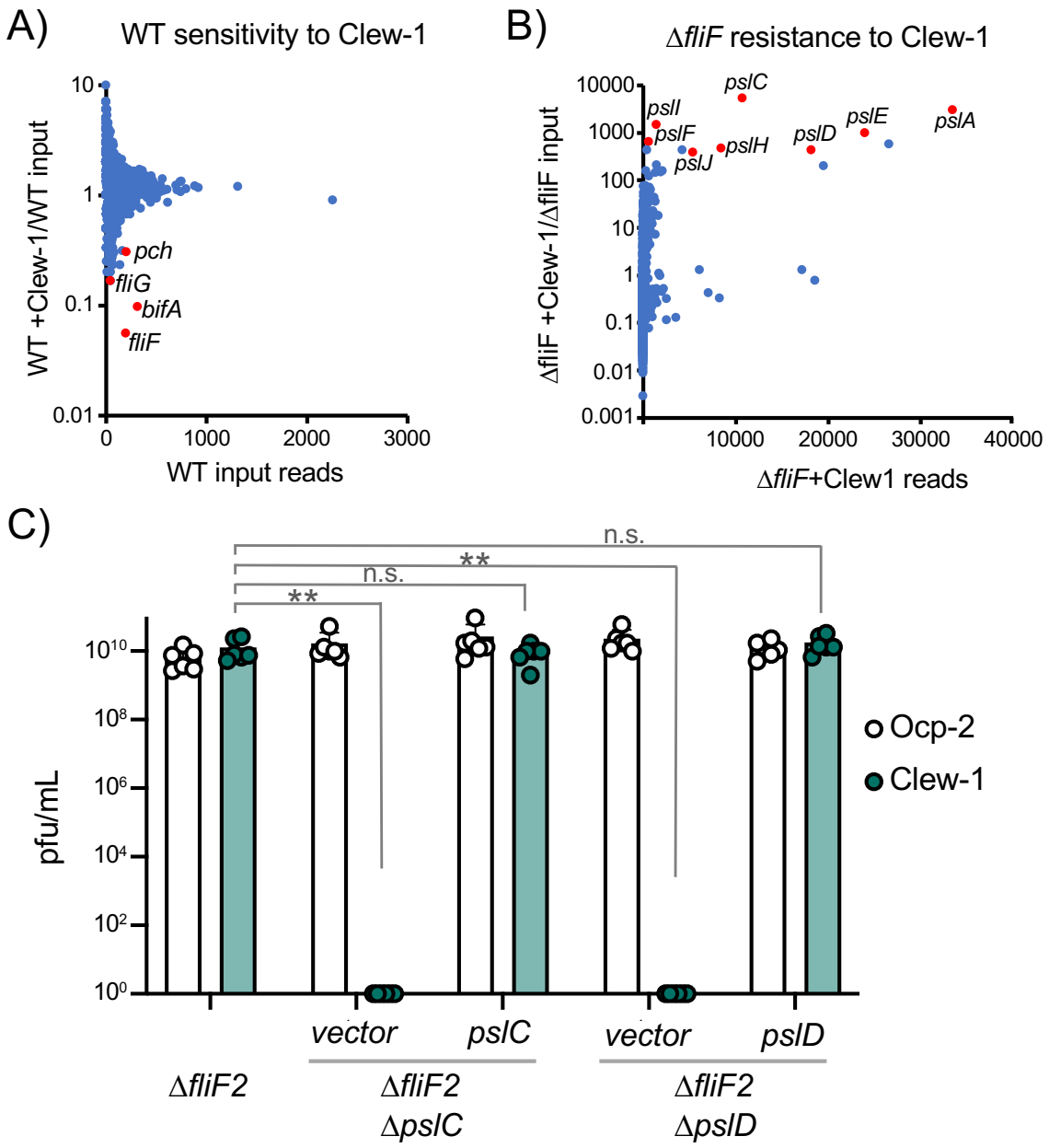
A)
WT sensitivity to Clew-1
WT +Clew-1/WT input
WT input reads
pch
fliG
bifA
fliF
B)
ΔfliF resistance to Clew-1
ΔfliF +Clew-1/ΔfliF input
ΔfliF+Clew1 reads
pslC
pslI
pslF
pslJ
pslH
pslD
pslE
pslA
C)
n.s.
**
n.s.
**
pfu/mL
Ocp-2
Clew-1
vector
pslC
vector
pslD
ΔfliF2
ΔfliF2
ΔpslC
ΔfliF2
ΔpslD

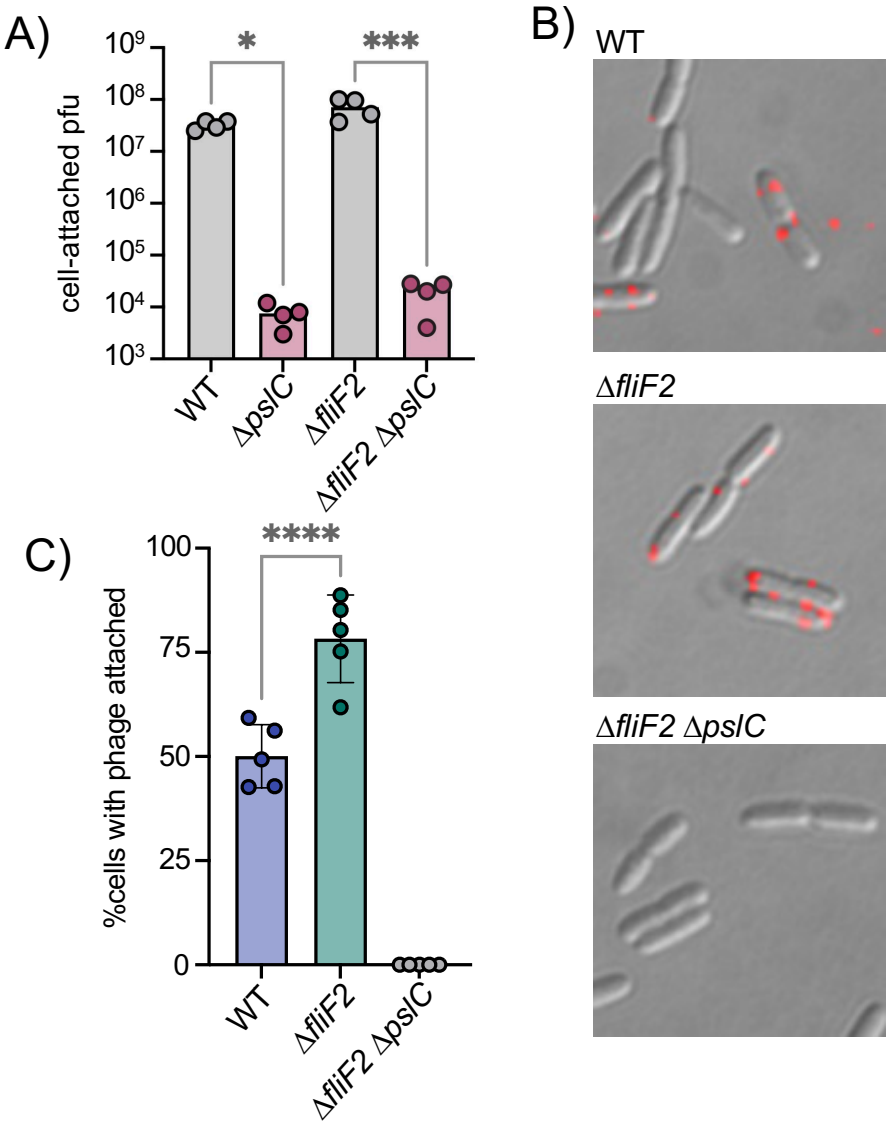
A)
cell-attached pfu
10^9
10^8
10^7
10^6
10^5
10^4
10^3
*
***
WT
ΔpslC
ΔfliF2
ΔfliF2 ΔpslC
B)
WT
ΔfliF2
ΔfliF2 ΔpslC
C)
%cells with phage attached
100
75
50
25
0
****
WT
ΔfliF2
ΔfliF2 ΔpslC

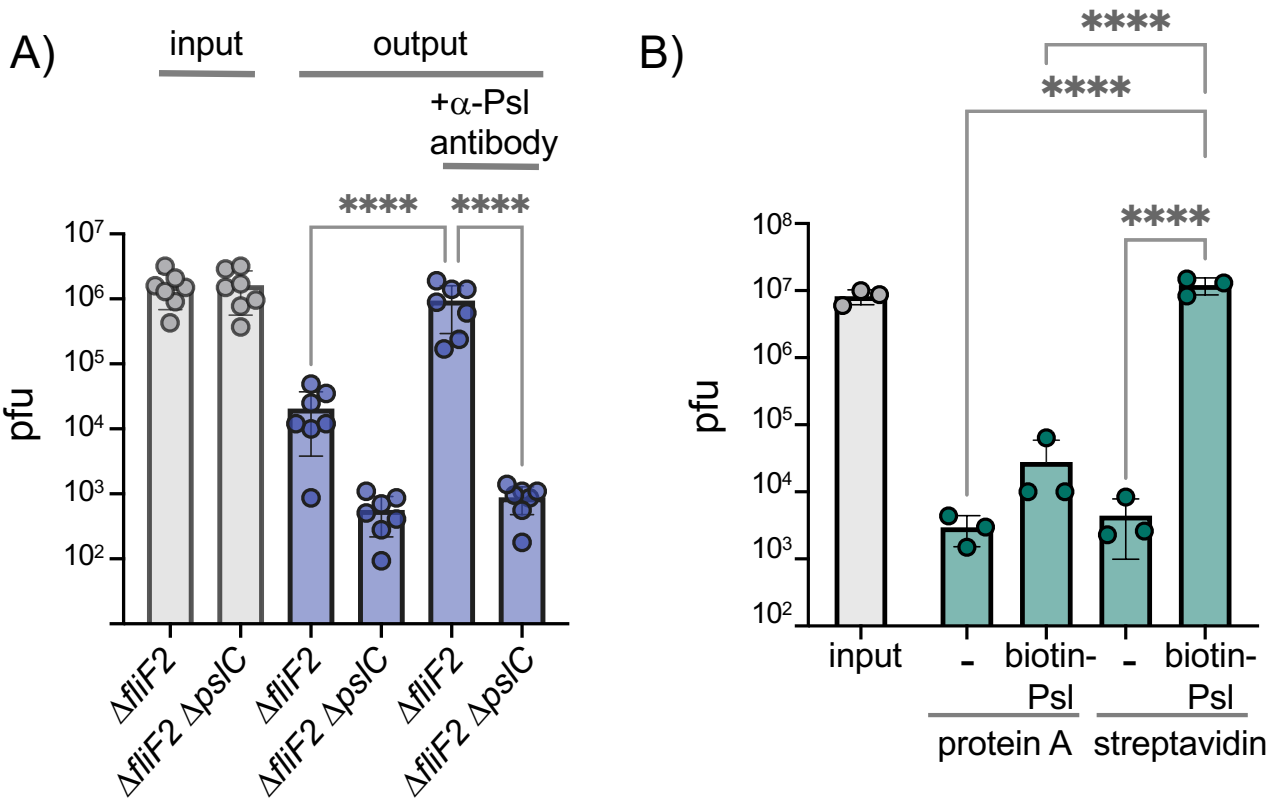
A)
input
output
+α-Psl antibody
****
****
pfu
10^7
10^6
10^5
10^4
10^3
10^2
ΔfliF2
ΔfliF2 ΔpslC
ΔfliF2
ΔfliF2 ΔpslC
ΔfliF2
ΔfliF2 ΔpslC
B)
****
****
****
pfu
10^8
10^7
10^6
10^5
10^4
10^3
10^2
input
-
biotin-Psl
-
biotin-Psl
protein A
streptavidin

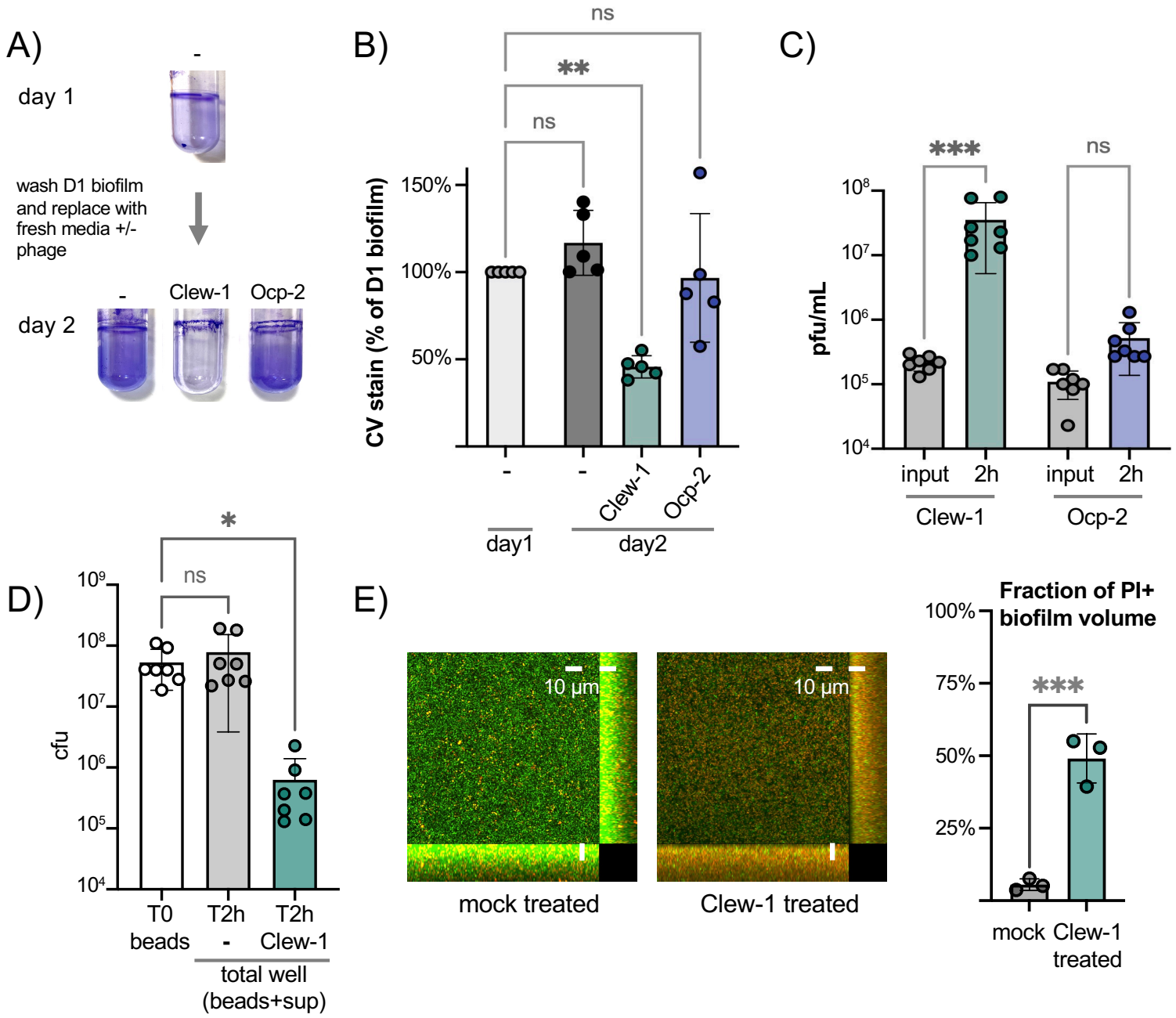
A)
-
day 1
wash D1 biofilm and replace with fresh media +/- phage
-
Clew-1
Ocp-2
day 2
B)
ns
**
ns
CV stain (% of D1 biofilm)
150%
100%
50%
-
-
Clew-1
Ocp-2
day1
day2
C)
***
ns
pfu/mL
10^8
10^7
10^6
10^5
10^4
input
2h
input
2h
Clew-1
Ocp-2
D)
*
ns
cfu
10^9
10^8
10^7
10^6
10^5
10^4
T0 beads
T2h -
T2h Clew-1
total well (beads+sup)
E)
10 µm
10 µm
mock treated
Clew-1 treated
Fraction of PI+ biofilm volume
100%
75%
50%
25%
***
mock
Clew-1 treated

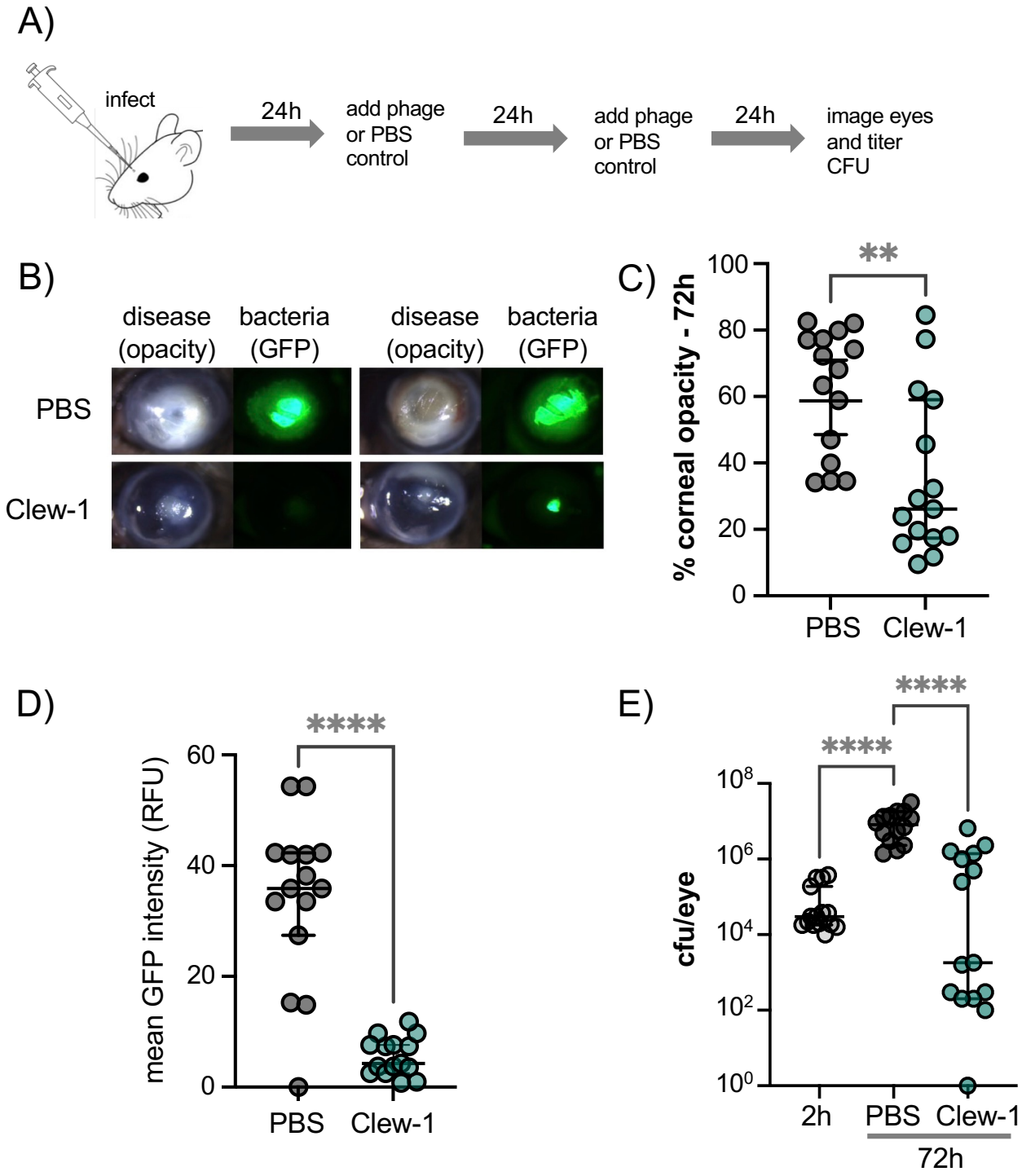
A)
infect
24h
add phage or PBS control
24h
add phage or PBS control
24h
image eyes and titer CFU
B)
disease (opacity)
bacteria (GFP)
disease (opacity)
bacteria (GFP)
PBS
Clew-1
C)
**
% corneal opacity - 72h
100
80
60
40
20
0
PBS
Clew-1
D)
****
mean GFP intensity (RFU)
60
40
20
0
PBS
Clew-1
E)
****
****
cfu/eye
10^8
10^6
10^4
10^2
10^0
2h
PBS
Clew-1
72h